

SUPPORTING INFORMATION

Solar thermochemical conversion of CO₂ into fuel via two-step redox cycling of non-stoichiometric Mn-containing perovskite oxides

Antoine Demont, Stéphane Abanades*

Processes, Materials, and Solar Energy Laboratory, PROMES-CNRS (UPR 8521), 7 Rue du Four Solaire, 66120 Font-Romeu, France

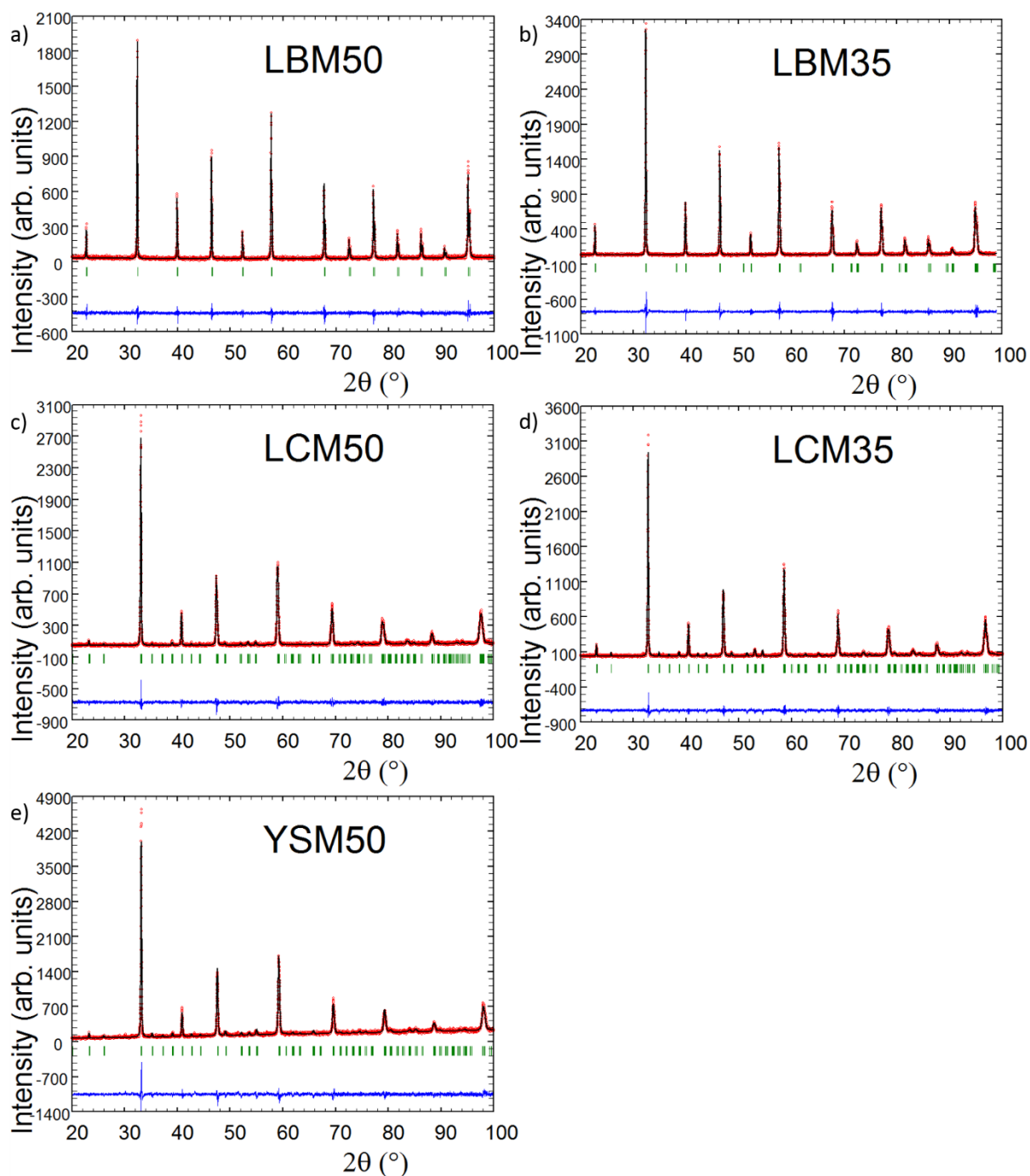


Figure S11: LeBail fits of powder X-ray diffraction data collected on A-site substituted perovskites. Experimental (red), calculated (black) and difference (blue) curves are shown.

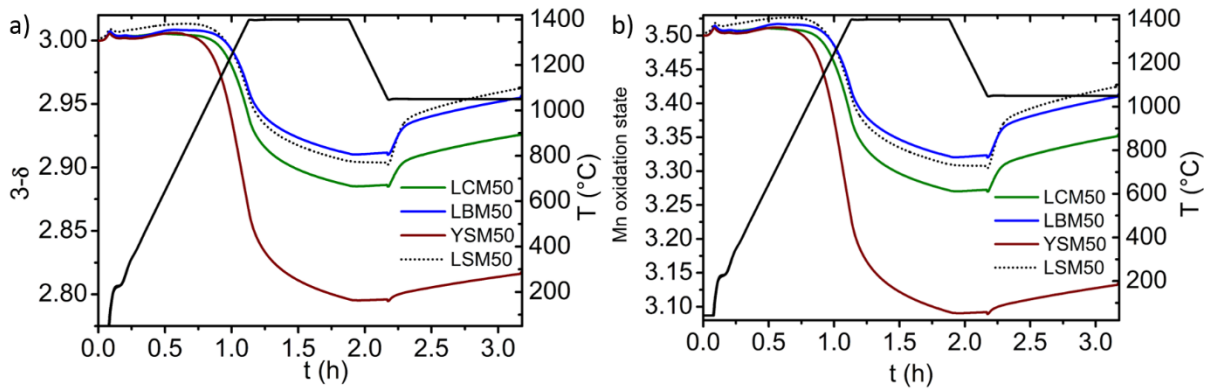


Figure S12: a) variation of the oxygen content ($3-\delta$) in LCM50, LBM50 and YSM50 during the first thermochemical cycle (reduction at 1400°C under Ar and re-oxidation at 1050°C under CO₂). b) variation of manganese formal oxidation state in LCM50, LBM50 and YSM50 during the first thermochemical cycle. The variations observed in LSM50 under the same conditions are shown on both graphs for comparison.

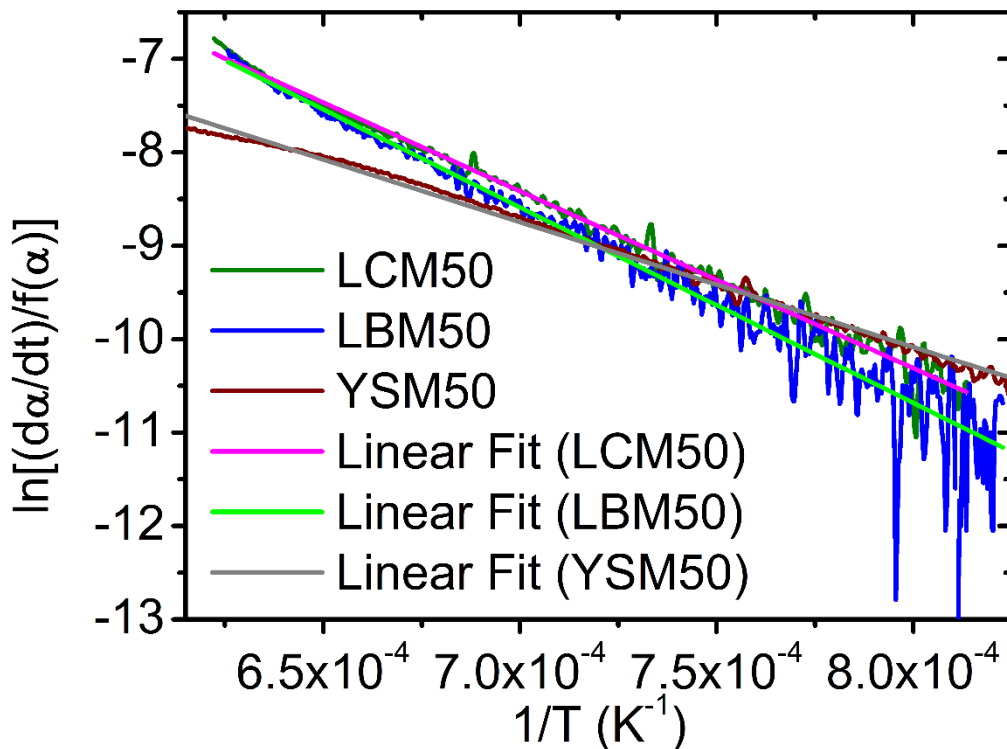


Figure S13: linear fits used to determine the activation energies for the reduction of LCM50, LBM50 and YSM50.

In order to determine the activation energies regarding the non-isothermal reduction step, the contracting sphere model was chosen. The conversion fraction α was determined as follows:

$$\alpha = (m_0 - m_t) / (m_0 - m_f)$$

where m_0 is the mass before the reduction, m_t is the mass at time t and m_f is the final mass at the end of the reduction step.

According to the contracting sphere model (constant rate of radial retraction of spherical reaction front as for the shrinking core model), the reaction model was expressed as:

$$f(\alpha) = 3(1 - \alpha)^{2/3}$$

The rate of a solid-state reaction can generally be described as:

$$d\alpha/dt = Ae^{-(E_a/RT)}f(\alpha)$$

where A is the pre-exponential factor (constant), E_a is the activation energy, T is the absolute temperature and R is the gas constant.

Therefore:

$$\ln[(d\alpha/dt)/f(\alpha)] = A - (E_a/R)(1/T)$$

and the plot of $\ln[(d\alpha/dt)/f(\alpha)] = f(1/T)$ (figures SI3 and SI4) gives access to E_a .

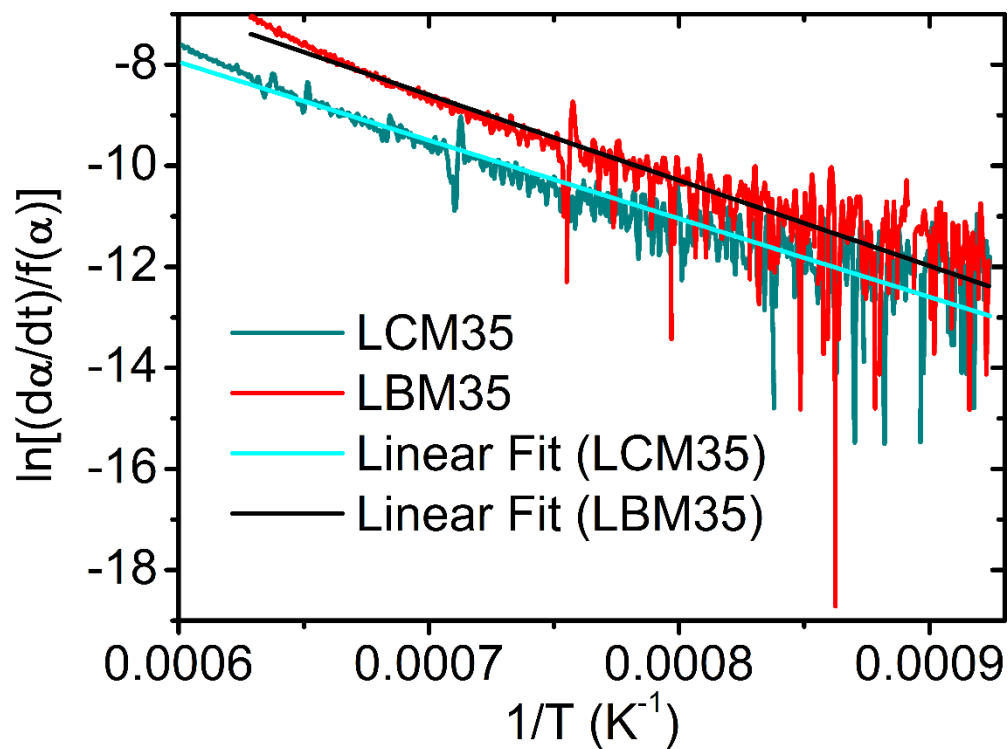


Figure SI4: linear fits used to determine the activation energies for the reduction of LCM35 and LBM35.

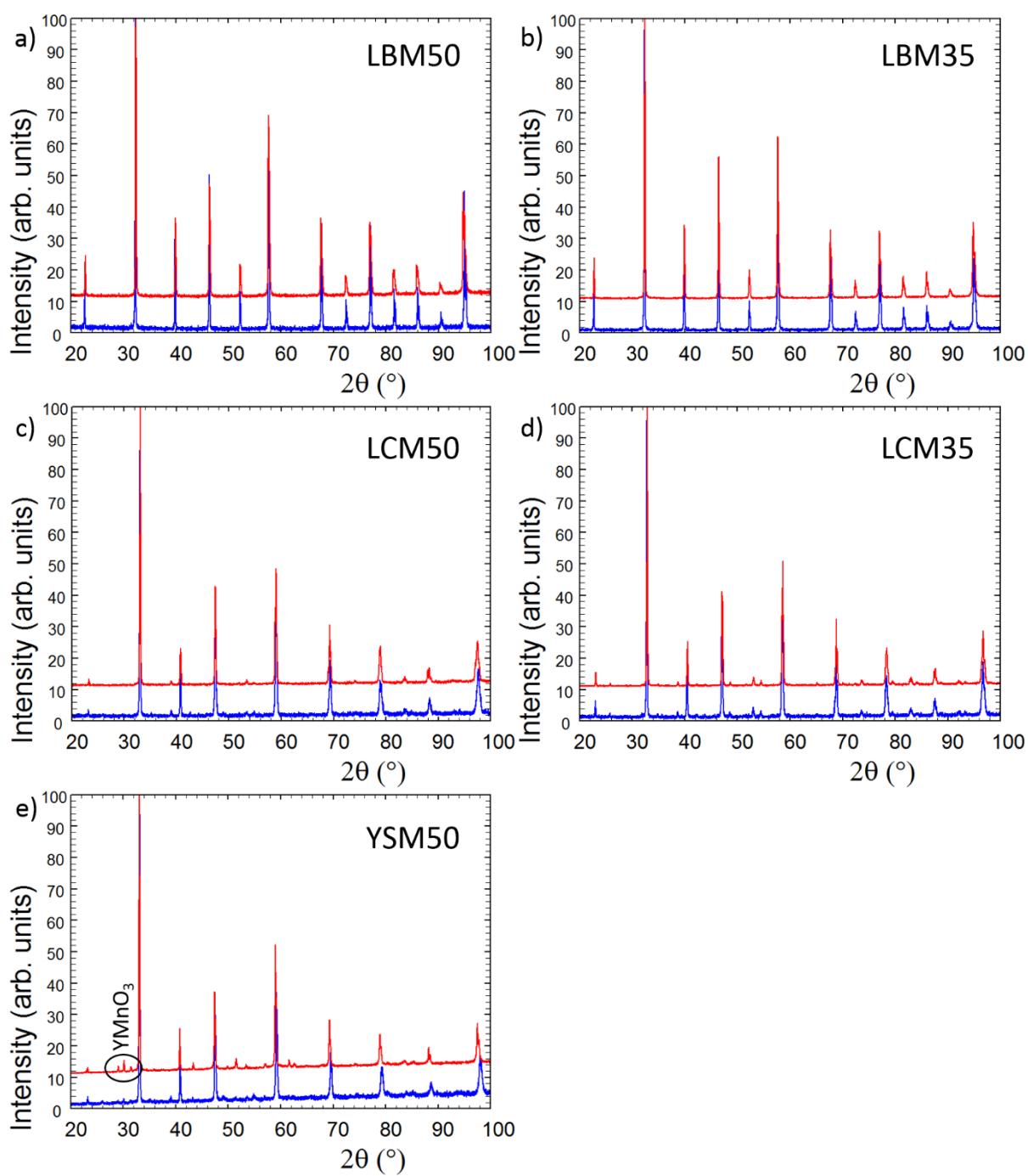


Figure S15: powder X-ray diffraction patterns collected on A-site substituted perovskites before (blue curve) and after (red curve) the thermochemical treatments.

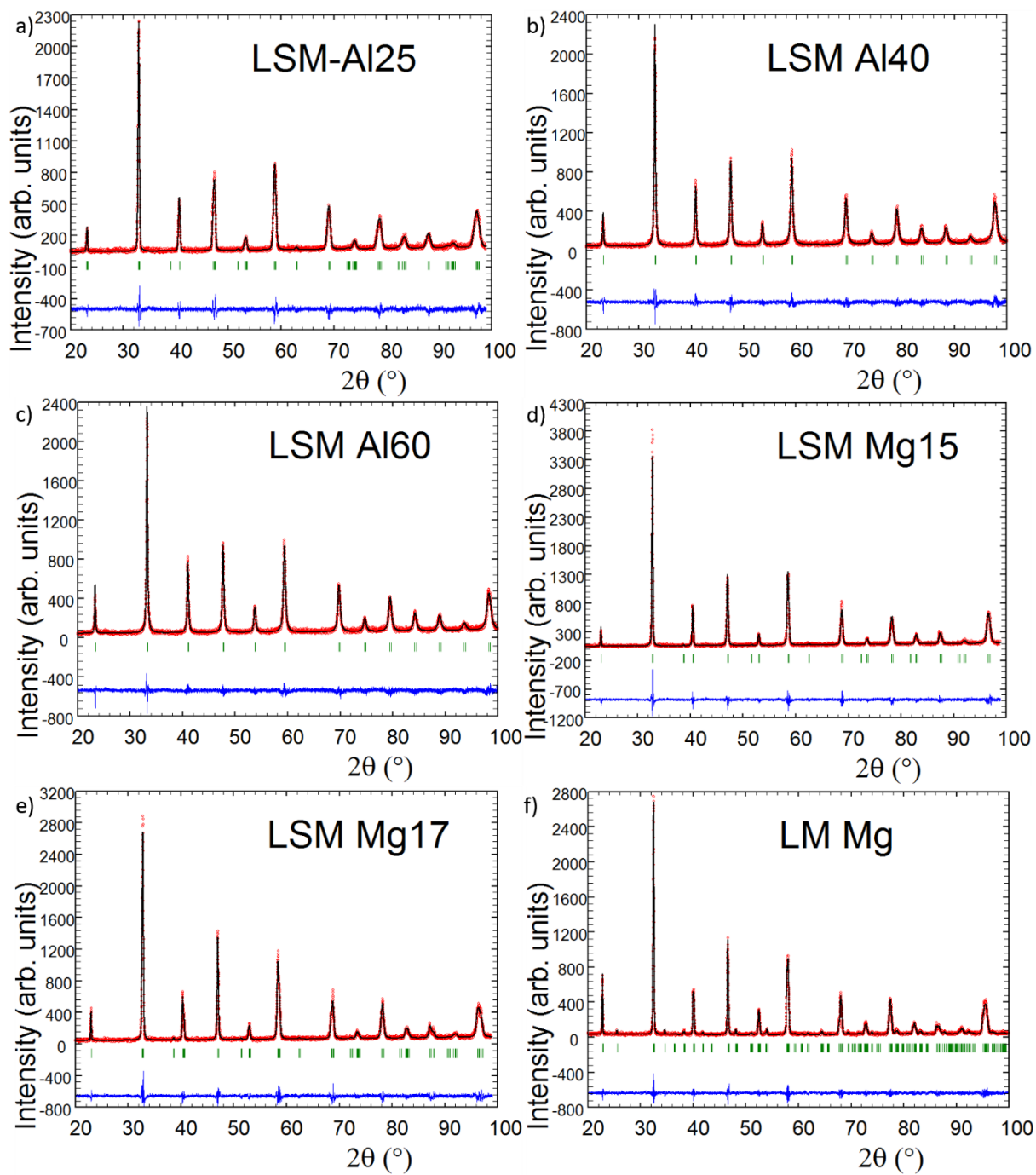


Figure S16: LeBail fits of powder X-ray diffraction data collected on B-site substituted perovskites. Experimental (red), calculated (black) and difference (blue) curves are shown.

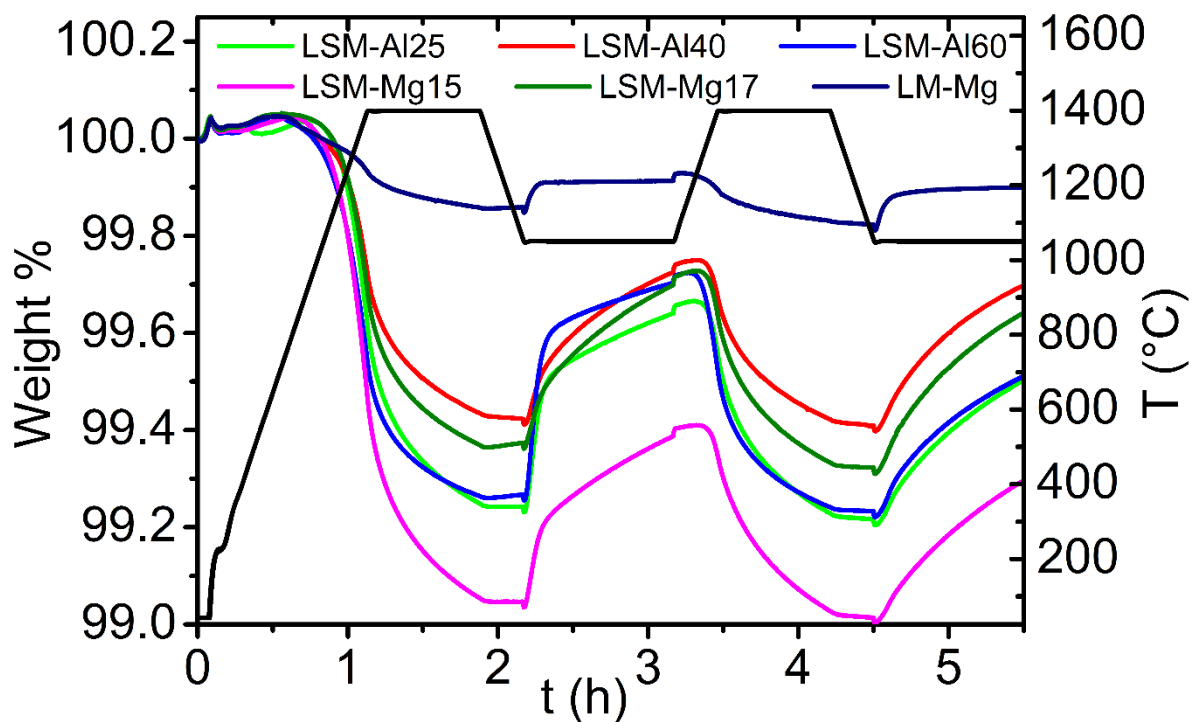


Figure S17: TG curves collected for B-site substituted perovskites during thermal reduction at 1400°C under Ar followed by exposure to CO₂ at 1050°C (2 cycles).

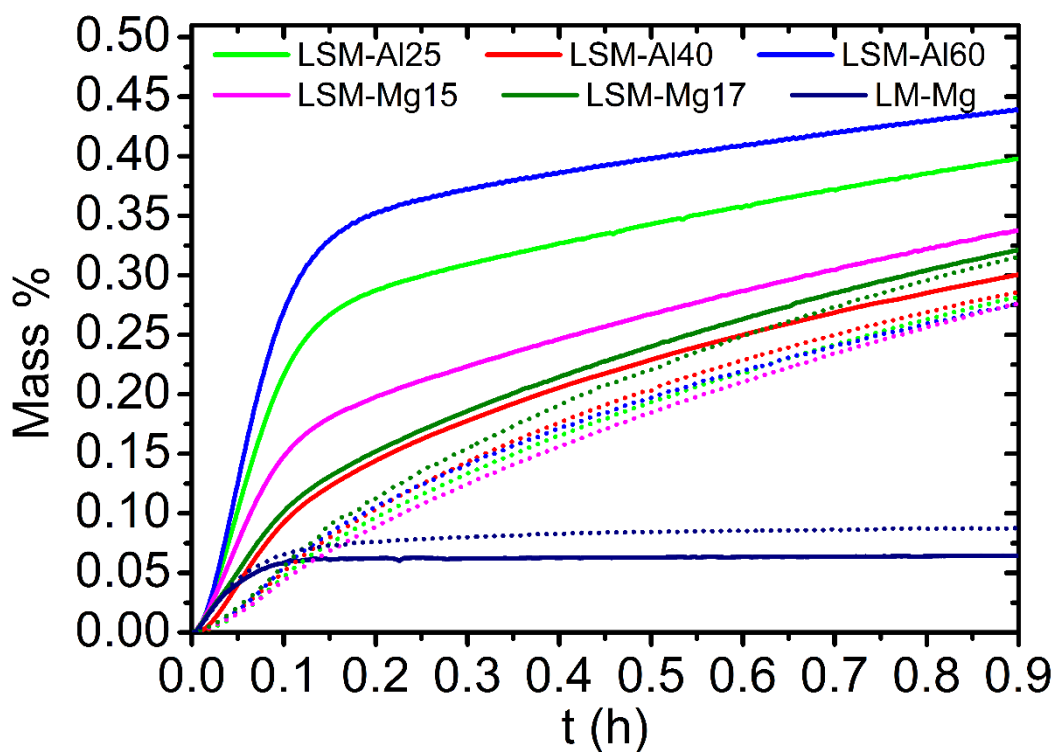


Figure S18: Mass variations measured following the thermal reduction step at 1400°C, during the re-oxidation under CO₂ at 1050°C for B-site substituted perovskites. The solid lines and the short spaced dots depict re-oxidation during the first and second thermochemical cycles respectively.

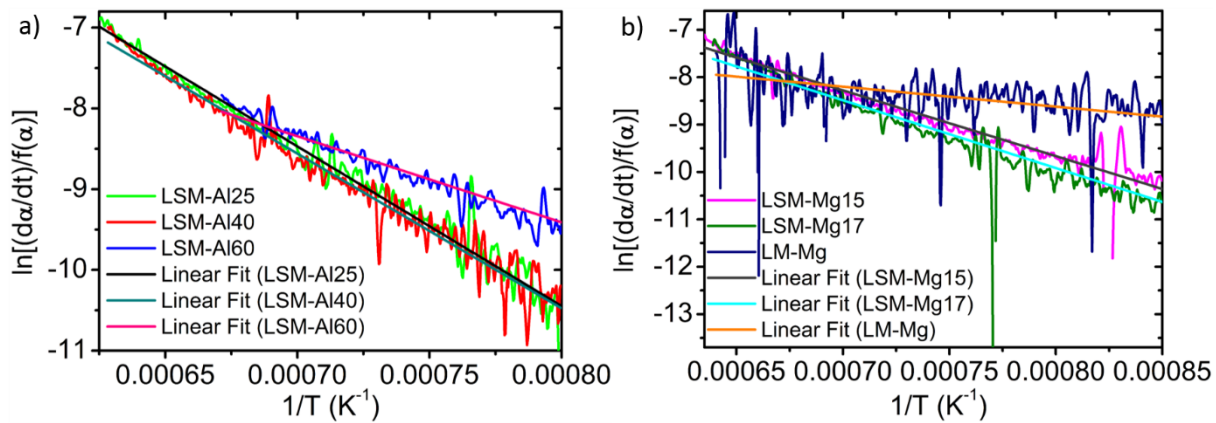


Figure S19: linear fits used to determine the activation energies for the reduction of B-site substituted perovskites. a) Al^{3+} -substituted perovskites. b) Mg^{2+} -substituted perovskites.

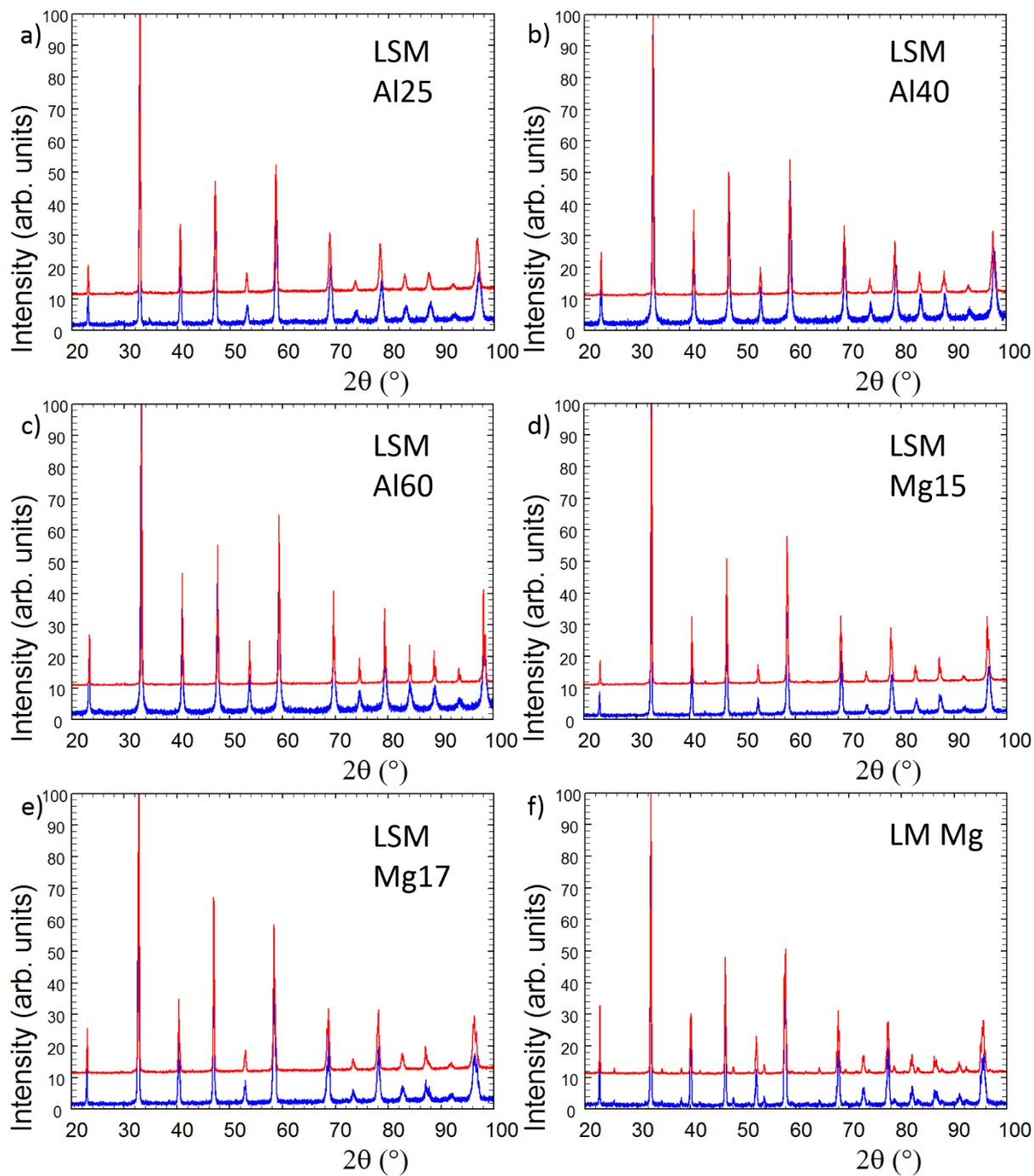


Figure S10: powder X-ray diffraction patterns collected on B-site substituted perovskites before (blue curve) and after (red curve) the thermochemical treatments.

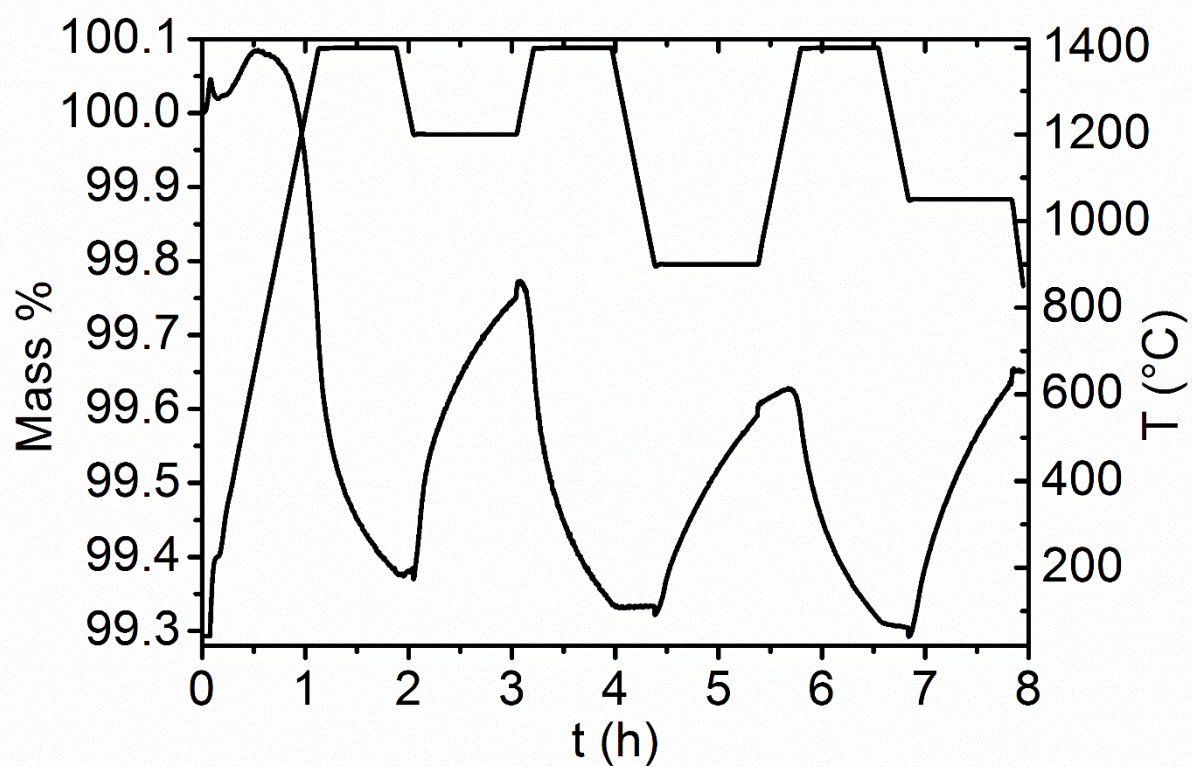


Figure S111: TG curves collected for LSM-Mg17 during thermal reduction at 1400°C under Ar followed by exposure to CO₂ at various temperatures.